PHYSICAL REVIEW B VOLUME 62, NUMBER 6 1 AUGUST 2000-II

Zener versus de Gennes ferromagnetism in $La_{1-x}Sr_xMnO_3$

J.-S. Zhou and J. B. Goodenough
Texas Materials Institute, ETC 9.102, University of Texas at Austin, Austin, Texas 78712-1063

(Received 20 March 2000)

Measurement of the transport properties of single-crystal $La_{0.86}Sr_{0.14}MnO_3$ as a function of temperature under different hydrostatic pressures $P \leqslant 18$ kbars has revealed a discontinuous change in the ferromagnetic Curie temperature T_c at $P \approx 3$ kbars where it crosses the first-order orbital-ordering transition, and at $P_c \approx 11$ kbars where it crosses a first-order transition from vibronic to metallic (Zener to de Gennes) ferromagnetism. On cooling below T_c within the vibronic phase, a second-order vibronic-insulator transition occurs at a T_{00} that increases with pressure to $P = P_c$; the first-order low-temperature insulator-metal transition is contiguous with the first-order vibronic-metallic transition occurring at $P_c \approx 11$ kbars. The distinction between Zener and de Gennes ferromagnetism in this system and the role of orbital ordering are clarified.

The manganese-oxide perovskites exhibit a colossal magnetoresistance (CMR) at the crossover from localized to itinerant electronic behavior. It is now generally recognized that the phenomenon is associated with an electron segregation into a more conductive ferromagnetic phase and a less conductive paramagnetic phase.[1] Double exchange has been widely invoked to explain the connection between charge transport and ferromagnetic order in these oxides, but the distinction between the original double-exchange model of Zener[2] and the de Gennes[3] formulation is rarely discussed; the Zener model has been ignored. In this paper, we demonstrate the existence of a distinguishable ferromagnetic phase found below the Curie temperature T_c for composition $0.1 < x < 0.2$ that lies between the type-*A* antiferromagnetic phase occurring below T_N for $0 \leqslant x < 0.1$ and a metallic ferromagnetic phase occurring for $x \geqslant 0.2$. We argue that the intermediate phase contains the two-manganese polarons originally envisaged by Zener; the metallic ferromagnetism found for $x \geqslant 0.2$ is well described by the de Gennes model. The Zener ferromagnetism is made possible by a short-range, dynamic orbital ordering at Mn(III) ions that was not envisaged by either Zener or de Gennes; dynamic, locally cooperative distortions introduce an isotropic ferromagnetic superexchange interaction between Mn(III) ions of the matrix[4] within which the Zener polarons move, and T_c increases sharply with the mobility of the Zener polarons since long-range double-exchange interactions depend on a polaron transfer time that is short relative to a spin-relaxation time.[5] Ordering of the Zener polarons orders the double-exchange interactions along the *c* axis and the superexchange interactions within the (001) basal planes. We show that the transition from a modified Zener to a de Gennes ferromagnetism is first order.

In the system $La_{1-x}Sr_xMnO_3$, the σ-bonding *e* orbitals are twofold degenerate, and the single-electron spin of a high-spin Mn(III) is coupled parallel to the localized spin of the t^3 configuration by a strong intra-atomic exchange. Cooperative orbital ordering at Mn(III) ions in $LaMnO_3$ removes the *e*-orbital degeneracy and localizes the *e* electrons to make $LaMnO_3$ an insulator; it also introduces ferromagnetic e^1-O-e^0 superexchange interactions between Mn(III) ions in the (001) planes that dominate the antiferromagnetic t^3-O-t^3 interactions; but along the *c* axis, the antiferromagnetic interactions prevail to give a type-*A* antiferromagnetic order below a Néel temperature T_N.[6] The long-range orbital ordering, which empties *e*-electron density along the *c* axis, transforms an O-orthorhombic structure with $c/\sqrt{2} > a$ into an O′-orthorhombic phase with $c/\sqrt{2} < a < b$. On heating above $T_{JT} = 750$ K, the long-range orbital ordering changes to short-range, dynamic orbital ordering in a conductive pseudocubic phase[7] that, on doping with Sr, becomes an O*-orthorhombic phase with $c/\sqrt{2} \leqslant b \leqslant a$.

T_{JT} decreases sharply with increasing *x*. Moreover, the time τ_h for an *e* electron of a Mn(III) to hop to a Mn(IV) near neighbor at the magnetic-ordering transition T_N or T_c decreases with increasing *x* from $\tau_h > \omega_0^{-1}$ for $x < 0.1$ to $\tau_h < \omega_0^{-1}$ for $x \geqslant 0.2$. A change at $x \approx 0.1$ from a second-order transition at T_N to a first-order transition at a ferromagnetic Curie temperature T_c signals stabilization below T_c of another conductive O* phase.[8,9] As τ_h / ω_0^{-1} decreases with increasing *x* in the interval $0.1 < x < 0.2$, T_c increases dramatically and crosses T_{JT} near $x = 0.15$. Moreover, a first-order transition from vibronic conduction ($\tau_h \approx \omega_0^{-1}$) to itinerant-electron behavior ($\tau_h < \omega_0^{-1}$) in an $x = 0.15$ crystal under pressure has been noted.[10] Okuda *et al.*[11] have identified the transition at an $x_c \approx 0.16$. On cooling below T_c in the vibronic phase, a transition at T_{00} to an insulator phase was originally postulated to signal an ordering of small-polaron Mn(IV) into alternate (001) planes on the basis of an observed *c*-axis structural modulation.[12] However, Endoh *et al.*[13] could find no evidence for small-polaron ordering, so they conjectured that it was an orbital-ordering transition.

Although careful studies of the phase diagram in the compositional range $0.1 < x < 0.2$ have been made on ceramic samples with compositional increments as small as $\Delta x = 0.005$,[14] the sensitivity of T_{JT}, T_c, T_{00} to *x* makes it difficult to monitor how T_c changes on crossing T_{JT} and $x_c(T)$ or how T_{00} approaches $x_c(T)$. We have circumvented this problem by studying the temperature variation of the resistivity $\rho(T)$ under different hydrostatic pressures $P \leqslant 18$ kbars of a single crystal of $La_{0.86}Sr_{0.14}MnO_3$. Hydrostatic pressure decreases the bending angle ϕ of the (180°-ϕ) Mn-O-Mn bonds, thereby decreasing ω_0^{-1}. In this respect, hydrostatic

0163-1829/2000/62(6)/3834(5)/$15.00

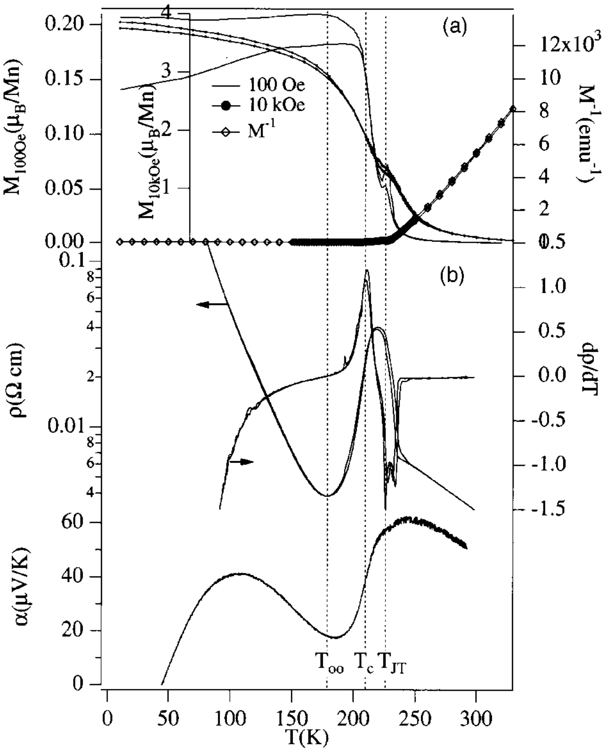

FIG. 1. (a) Magnetization in an applied $H = 100$ Oe and 10 kOe, $\chi(T)^{-1}$ in 10 kOe and (b) resistivity $\rho(T)$, $d\rho/dT$, and thermoelectric power $\alpha(T)$ for single-crystal $La_{0.86}Sr_{0.14}MnO_3$.

pressure is equivalent to increasing x, but without changing the chemical composition; it increases T_c, lowers T_{JT}, and decreases $x_c(T)$.[8–10,15] The single-crystal composition $x = 0.14$ was chosen because, under ambient pressure, T_{JT} lies about 20 K above T_c. The transition at $T_{00} = 190$ K is second order in this crystal, whereas it is first order at $x = 0.12$, changing smoothly to second order with increasing x and pressure.[10,12] Neutron-diffraction data[12] have shown that the structure below T_{00} is identical whether the transition is first or second order.

The $La_{0.86}Sr_{0.14}MnO_3$ crystal, grown in an image furnace, was first characterized under ambient pressure. The critical temperatures T_{JT}, T_c, and T_{00} evident in the data of Fig. 1 are the same as those reported for $x = 0.14$ polycrystalline samples.[14] In Fig. 1(a), the magnetization obtained in a magnetic field $H = 100$ Oe shows an anomaly in the paramagnetic phase at T_{JT} similar to that observed at T_{JT} in $LaMnO_3$;[7] the $\chi(T)^{-1}$ data for the O* phase exhibits a Curie-Weiss behavior with a θ near T_{JT}. It appears that the transition to the orbitally ordered O′ phase suppresses the onset of ferromagnetism about to occur at a $T_c(\mathrm{O}^*) \approx T_{JT}$, lowering the measured $T_c(\mathrm{O}')$ that occurs in the O′ phase. The transitions in the $\rho(T)$ data of Fig. 1(b) are much sharper than those found in polycrystalline samples. On cooling, the resistivity shows a sharp upturn at T_{JT} and T_{00}, a downturn at T_c. The transition at T_{JT} is abrupt and has a thermal hysteresis characteristic of a first-order phase change. However, the derivative analysis $d\rho/dT$ of the transition at T_{JT} shows two minima. The higher-temperature transition is discernible as a small shoulder on the lower-temperature peak in the 100-Oe magnetization data. We identify T_{JT} with the lower-temperature minimum in $d\rho/dT$, and we use this feature to identify T_{JT} in our high-pressure experiments. Similarly, the sharp maximum in $d\rho/dT$, which corresponds to a dramatic increase in $\chi(T)$, is used to label the ferromagnetic Curie temperature; it is associated with a sharp decrease in $\rho(T)$ on cooling through T_c. We define T_{00} as the temperature where $\rho(T)$ exhibits a minimum below T_c. The temperature dependence of the thermoelectric power $\alpha(T)$ of Fig. 1(b) shows important changes in the concentrations of mobile charge carriers at T_c and T_{00}, but not at T_{JT}. Finally, Fig. 1(a) shows a difference in the magnetization below T_c between values obtained on heating after cooling in the measuring field [field cooled (FC)] and in zero magnetic field [zero field cooled (ZFC)]. The magnetization in $H = 10$ kOe approaches the theoretical spin-only value of $3.86\mu_B$/Mn, but the shape of the $M(T)$ curve in 100 Oe is similar to that of a spin glass, which is evidence of two magnetic phases below T_c in low magnetic fields. There is no anomaly in the magnetization at T_{00}.

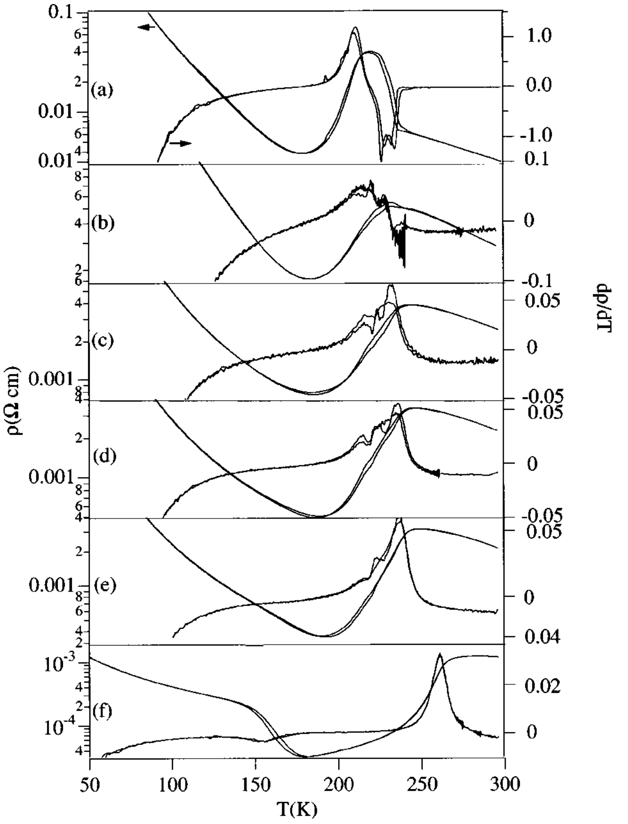

FIG. 2. Resistivity $\rho(T)$ and $d\rho/dT$ for single-crystal $La_{0.86}Sr_{0.14}MnO_3$ under different hydrostatic pressures, (a) 1 bar, (b) 2.5 kbars, (c) 4.8 kbars, (d) 6.5 kbars, (e) 7.3 kbars, and (f) 14.0 kbars.

Our high-pressure experiments were performed with a correction for the pressure variation with temperature as described elsewhere.[10] The pressure in the self-clamped cell was changed at room temperature. Moreover, measurements were also carried out after reducing the pressure at room temperature from 18 kbars to different values in order to determine any pressure hysteresis. After total release of the pressure, measurements were again taken on the same crystal with increasing pressure; the initial results were duplicated precisely, which demonstrated that no permanent change occurred in the crystal during the pressure and temperature cycling.

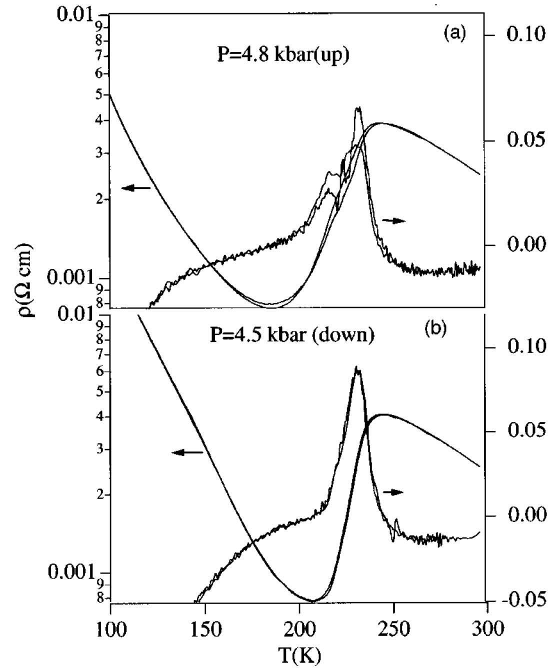

FIG. 3. Comparison of $\rho(T)$ and $d\rho/dT$ for single-crystal $La_{0.86}Sr_{0.14}MnO_3$ on (a) increasing pressure from ambient to 4.8 kbar, (b) decreasing pressure from 18 kbars to 4.5 kbars.

Figure 2 illustrates typical changes in $\rho(T)$ and $d\rho/dT$ with pressure. T_{JT} and T_c are clearly separated at $P = 1$ bar, Fig. 2(a). At $P = 2.5$ kbars, Fig. 2(b), the structural and magnetic transitions overlap. Figure 2(c) shows that the crossover of T_{JT} and T_c is completed at 4.8 kbars. However, the structural change on cooling through T_{JT} does not cause an upturn in $\rho(T)$ where it occurs below T_c; the orbital ordering below $T_{JT} < T_c$ retains a long c-axis Mn-O bond characteristic of an O* rather than an O′ structure, and $\rho(T)$ continues to decrease sharply with decreasing temperature. However, the first-order character of the transition at T_{JT} is retained. With a further increase in pressure, T_c continues to increase and T_{JT} to decrease; the structural transition at T_{JT} retains its first-order character, whereas the transition at T_c changes smoothly from first to second order near $P = 11$ kbars. T_{00} increases with pressure until a critical pressure $P_c \approx 11$ kbars, where it merges with a sharply decreasing first-order insulator-metal transition at T_{IM}. Figure 2(f) is typical of the $\rho(T)$ curves found for $P > P_c$. At these pressures, a sharp drop in $\rho(T)$ on cooling through T_c is followed by a moderate change with temperature over a broad range $T_{IM} < T < T_c$ and the double minimum associated with T_{JT} is suppressed.

Although complete release of pressure at room temperature restores the crystal to its original state, the $\rho(T)$ curves obtained with increasing and decreasing pressure showed a large hysteresis. Figure 3 shows the $\rho(T)$ curves taken under similar pressures: $P = 4.8$ kbars for increasing pressure and 4.5 kbars for decreasing pressure. T_c is the same for both curves, but $T_{JT} > T_{00}$ for increasing pressure becomes $T_{JT} = T_{00}$ at an intermediate temperature on reducing the pressure. This pressure hysteresis disappears for $P < 4$ kbars where T_{JT} and T_{00} become separate.

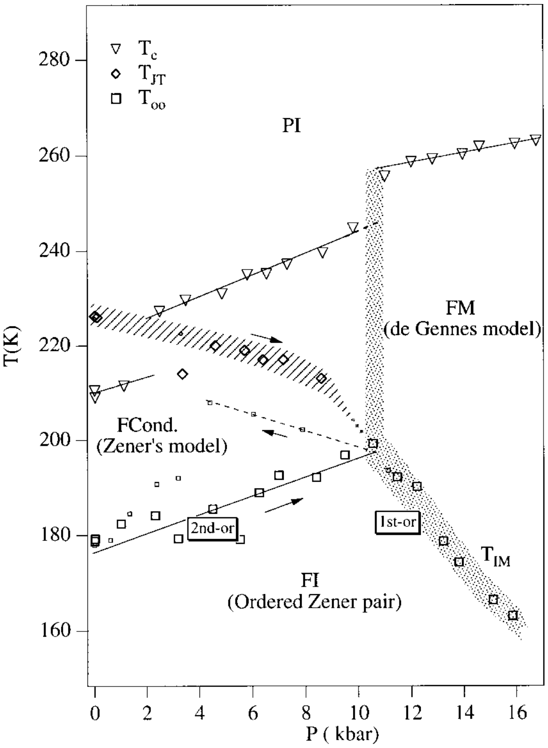

FIG. 4. Pressure-temperature phase diagram below room temperature for $La_{0.86}Sr_{0.14}MnO_3$. The lines are guides to the eye.

The phase diagram of Fig. 4 summarizes the pressure variations of the critical temperatures. (a) T_c increases sensitively with hydrostatic pressure. (b) T_c jumps discontinuously as it crosses T_{JT} and $P \approx 11$ kbars; the jump at $P_c \approx 11$ kbars signals a first-order electronic phase change at P_c and is to be distinguished from the jump where T_c crosses the O*-R transition temperature.[14] (c) The slope dT_c/dP changes at P_c. (d) T_{00} increases with pressure as does T_c until it reaches its maximum value of 198 K at $P_c \approx 11$ where it meets the vibronic-itinerant electronic transition occurring at P_c and the insulator-metal transition at T_{IM}. T_{IM} falls sharply with increasing pressure. (e) With decreasing pressure, a maximum $T_{00} = T_{JT} = 208$ K was found at 4 kbars. (f) Where T_{00} meets T_{IM}, the transition changes abruptly from second to first order. (g) The system remains ferromagnetic below T_c on crossing T_{JT}, T_{00}, and T_{IM}/P_c. (h) The structural change at T_{IM}/P_c appears to be primarily a volume contraction, but static oxygen displacements in the (001) planes of the charge-density wave (CDW) phase disappear on crossing T_{IM}.[14]

To interpret Fig. 4, we begin with a review of the ferromagnetic double-exchange interaction for a mixed-valent system. It involves a rapid real charge transfer of an e electron that preserves the spin angular momentum; a large intra-atomic exchange interaction favors ferromagnetic alignment of the mobile e-electron spin with the localized spins $S = \frac{3}{2}$. Zener postulated fast electron transfer from Mn(III) to oxygen and a same-spin oxygen electron to the Mn(IV) within a Mn(III)-O-Mn(IV) pair; hence, the term double exchange. The pairs were assumed to diffuse with a mobility $\mu_p = eD_0/kT$, where the diffusion coefficient had a motional enthalpy $\Delta H_m = 0$ in order to account for the metallic temperature dependence of $\rho(T)$ and the long-range ferromagnetic order. This model implies a $\tau_h \approx \omega_0^{-1}$. The de Gennes model, on the other hand, introduced itinerant *e* electrons having a tight-binding bandwidth $W=2zb\cos(\theta_{ij}/2)$, where $z=6$ is the number of Mn near neighbors, *b* is the spin-independent Mn-O-Mn resonance integral, and θ_{ij} is the angle between localized spins on Mn near neighbors. The de Gennes model appears to be appropriate for the metallic ferromagnetic (FM) phase found at $P>11$ kbars. The problem is to account for the ferromagnetism found below T_c for $P<11$ kbars, and in particular below T_{00} where there is no long-range rapid motion of the charge carriers. To address this problem, we must consider the *e*-orbital ordering.

In the O* phase with $c/\sqrt{2}\leqslant b\leqslant a$ at temperatures $T>T_{JT}$, the orbital ordering is short range and dynamic. The hole mobility should be nearly isotropic in this case. Measurements of $\alpha(T)$ on $(La_{1-y}Nd_y)_{0.7}Ca_{0.3}MnO_3$ samples have allowed us to identify the presence of two-manganese polarons in the paramagnetic phase.[16] Fast electron transfer within a Mn(III)-O-Mn(IV) pair would give a superparamagnetic, two-manganese Zener polaron. Moreover, the CMR phenomenon indicates the presence of a more conductive minority phase within a less conductive matrix, and the $\alpha(T)$ data showed a progressive trapping out of the Zener polarons from the matrix phase with decreasing $T>T_c$. In our $x=0.14$ sample, the continuity in $\alpha(T)$ at ambient pressure on cooling through $T_{JT}>T_c$ indicates there is no discontinuity in the number of mobile polarons on traversing the first-order orbital-ordering transition at T_{JT}; an orbital ordering that introduces an anisotropy in the mobility does not change the statistical contribution to $\alpha(T)$. However, there is a return to another O* phase on cooling through T_c, and a sharp decrease in $\rho(T)$ and $\alpha(T)$ indicates a dramatic increase in the concentration of mobile charge carriers on cooling through T_c. This change has been interpreted to signal growth of a more conductive, hole-rich minority phase to beyond its percolation threshold,[1] and the evidence for spin-glass behavior below T_c in lower fields supports a two-phase model. The O* phase below T_{JT} is to be distinguished from that above T_{JT}, which is why an O*-O* transition is found at a $T_{JT}<T_c$ above $P=3$ kbars. The O* phase in the range $T_{00}<T<T_{JT}$ with $T_{JT}<T_c$ is conductive, which means that the Zener polarons are mobile even though an orbital ordering has occurred. Dynamic fluctuations of the occupied *e* orbitals must be present even if preferentially ordered into the (001) planes. On the other hand, a relatively long *c* axis indicates the axes of the Zener polarons are preferentially ordered along the *c* axis. The jump in T_c at its crossover with T_{JT} is consistent with more isotropic double-exchange and ferromagnetic superexchange contributions in the O* phase above T_{JT}. The jump in T_c at $P\approx 11$ kbars reflects a stronger long-range double-exchange contribution on changing from vibronic to itinerant charge carriers. The change in slope of T_c vs P at P_c is consistent with a change from a Zener double-exchange plus superexchange phase to a de Gennes double-exchange phase. Significantly, there is also an abrupt decrease in the oxygen isotope effect on T_c near this crossover.[15,17]

Fast *e*-electron transfer within a Zener polaron requires orientation of the charge density along the axis of the polaron. A low $\rho(T)$ and $\alpha(T)$ below T_c signals long-range mobility of the polarons in the ferromagnetic, vibronic phase with a $\tau_h\approx\omega_0^{-1}$ for the holes to change from one Mn(III) near-neighbor partner to another to produce a polaron mobility; a $\tau_h<\omega_0^{-1}$ occurs between ferromagnetically coupled partners of a polaron. Retention of good conductivity and ferromagnetic order below $T_{JT}<T_c$ is consistent with retention of either isotropic ferromagnetic superexchange and double-exchange interactions or a progressive ordering of ferromagnetic superexchange interactions within (001) planes and double-exchange interactions along the *c* axis. The former situation applies above T_{JT}. Therefore, we suggest that the orbital ordering below a $T_{JT}<T_c$ represents the onset of a preferred orientation of Zener pairs along the *c* axis in response to basal-plane ordering of the Mn(III) orbitals not involved in Zener polarons. Below T_{00}, the orbital ordering becomes stabilized into a static CDW in which the Zener polarons become trapped with their axes oriented along the *c* axis so as to create a greater hole density in alternate (001) planes. Ordering into a static CDW below T_{00} is consistent with the observation of a *c*-axis modulation and a suppression of the polaron mobility[12] as well as the failure to find evidence for the Mn(IV)-ion ordering into alternate (001) planes.[13] Stationary Zener polarons with their axes oriented along the *c* axis introduce *c*-axis double-exchange and a longer *c* axis compatible with an O* structure: A Hartree-Fock calculation by Mizokawa Khomskii, and Sawatzky[18] also orders charge along the *c* axis to obtain ferromagnetism below T_{00}. Orbital ordering within (001) planes at the Mn(III) ions not involved in Zener pairs would give basal-plane ferromagnetic superexchange interactions as in the parent compound $LaMnO_3$. An intimate relation between T_{JT} and T_{00} is demonstrated by the pressure hysteresis. On lowering the pressure from 18 kbars to a $P\geqslant 4$ kbars at room temperature, a $T_{00}=T_{JT}$ is intermediate between the T_{00} and T_{JT} found on increasing the pressure from ambient. This behavior suggests that at $P=18$ kbars at room temperature, the axes of the Zener polarons are oriented along the *c* axis and the pressure hysteresis is associated with an order-disorder *c*-axis orientation of the Zener polarons in the paramagnetic phase at room temperature. Pressure stabilization of the *c*-axis orientation of the Zener polarons is compatible with a continuous increase in T_{00} with pressure, whereas T_{00} reaches a maximum in the range $0.14<x<0.15$ at ambient pressure.

In conclusion, pressure experiments on a single crystal with a carefully selected composition $x=0.14$ have allowed us to demonstrate/propose the following: (1) A discontinuous increase in T_c occurs at $P\approx 3$ kbars where T_c crosses the orbital-ordering transition temperature T_{JT} and also at $P_c\approx 11$ kbars where T_c crosses a vibronic-itinerant electronic transition. (2) In the range $T_{00}<T<T_c$ and $3<P<P_c\approx 11$ kbars, the vibronic phase contains a ferromagnetic double-exchange contribution from mobile Zener polarons together with a ferromagnetic Mn(III)-O-Mn(III) superexchange coupling that is made isotropic by locally cooperative, dynamic Jahn-Teller deformations. We designate this phase a modified-Zener double-exchange ferromagnet. (3) Below T_{JT}, orbital ordering introduces ferromagnetic superexchange interactions in the (001) planes, but the magnetic order is antiferromagnetic below a T_N unless Zener polarons are present with axes oriented parallel to the *c* axis; these

polarons become trapped in a static charge-density wave below a $T_{00} \leqslant T_{JT}$. (4) At a $P > 11$ kbars and $T_{IM} < T < T_c$, itinerant σ^* electrons of *e*-orbital parentage result in a de Gennes ferromagnetism. (5) At room temperature, a pressure $P = 18$ kbars orients the axes of the Zener polarons along the *c* axis, and this orientation is retained on removal of the pressure down to 4 kbars. This hysteresis is reflected at low temperatures in a pressure hysteresis of T_{JT} and T_{00} in the range $4 < P < 11$ kbars.

Note added in proof. Recently, Dai *et al.*[20] have reported neutron scattering data on several ferromagnetic manganese perovskites with a reduced T_c that show a strong magnon coupling to optical phonons. On the other hand, this coupling becomes negligible in manganese perovskites having a higher Curie temperature. A strong magnon-phonon coupling would be a consequence of the modified Zener double-exchange ferromagnetism proposed in this paper.

We thank A. Asamitsu and Y. Tokura for providing the single-crystal sample,[19] and the NSF, the Robert A. Welch Foundation, and the TCSUH of Houston, Texas for financial support.

---

[1] J. B. Goodenough, Aust. J. Phys. **52**, 155 (1999); A. Moreo, S. Yunoki, and E. Dagotto, Science **283**, 2034 (1999); J. B. Goodenough and J.-S. Zhou, Nature (London) **386**, 229 (1997).

[2] C. Zener, Phys. Rev. **82**, 403 (1951).

[3] P.-G. de Gennes, Phys. Rev. **118**, 141 (1960).

[4] J. B. Goodenough, A. Wold, R. J. Arnott, and N. Menyuk, Phys. Rev. **124**, 373 (1961).

[5] J. B. Goodenough, J. Appl. Phys. **81**, 5330 (1997).

[6] J. B. Goodenough, Phys. Rev. **100**, 564 (1955).

[7] J.-S. Zhou and J. B. Goodenough, Phys. Rev. B **60**, R15 002 (1999).

[8] W. Archibald, J.-S. Zhou, and J. B. Goodenough, Phys. Rev. B **53**, 14 445 (1996).

[9] J.-S. Zhou, W. Archibald, and J. B. Goodenough, Nature (London) **381**, 770 (1996).

[10] J.-S. Zhou, J. B. Goodenough, A. Asamitsu, and Y. Tokura, Phys. Rev. Lett. **79**, 3234 (1997).

[11] T. Okuda, A. Asamitsu, Y. Tomioka, T. Kimura, Y. Taguchi, and Y. Tokura, Phys. Rev. Lett. **81**, 3203 (1998).

[12] Y. Yamada, O. Hino, S. Nohdo, R. Kanao, T. Inami, and S. Katano, Phys. Rev. Lett. **77**, 904 (1996).

[13] Y. Endoh, K. Hirota, S. Ishihara, S. Okamoto, Y. Murakami, A. Nishizawa, T. Fukuda, H. Kimura, H. Nojiri, K. Kaneko, and S. Maekawa, Phys. Rev. Lett. **82**, 4328 (1999).

[14] B. Dabrowski, X. Xiong, Z. Bukowski, R. Dybzinski, P. W. Klamut, J. E. Siewenie, O. Chmaissem, J. Shaffer, C. W. Kimball, J. D. Jorgensen, and S. Short, Phys. Rev. B **60**, 7006 (1999).

[15] J.-S. Zhou and J. B. Goodenough, Phys. Rev. Lett. **80**, 2665 (1998).

[16] J. B. Goodenough and J.-S. Zhou, in *Epitaxial Oxide Thin Films III*, edited by D. G. Schlom *et al.*, Mater. Res. Soc. Symp. Proc. No. 474 (Materials Research Society, Pittsburgh, 1998), p. 335.

[17] G. M. Zhao, K. Conder, H. Keller, and K. A. Müller, Nature (London) **381**, 676 (1996).

[18] T. Mizokawa, D. I. Khomskii, and G. A. Sawatzky, Phys. Rev. B **61**, R3776 (2000).

[19] A. Urushibara, Y. Moritomo, T. Arima, A. Asamitsu, G. Kido, and Y. Tokura, Phys. Rev. B **51**, 14 103 (1995).

[20] Pengcheng Dai, H. Y. Hwang, Jiandi Zhang, J. A. Fernandez-Baca, S.-W. Cheong, C. Kloc, Y. Tomioka, and Y. Tokura, Phys. Rev. B **61**, 9553 (2000).